

# Preparation of Imprinted Polymers at Surface of Magnetic Nanoparticles for the Selective Extraction of Tadalafil from Medicines

Yun Li,<sup>†</sup> Mei-juan Ding,<sup>†</sup> Shu Wang, Ruo-yu Wang, Xiao-li Wu, Ting-ting Wen, Li-hua Yuan, Peng Dai, Yu-hui Lin, and Xue-min Zhou\*

School of Pharmacy, Nanjing Medical University, Nanjing City 210029, P.R. China

 Supporting Information

**ABSTRACT:** In this paper, highly selective core–shell molecularly imprinted polymers (MIPs) of tadalafil on the surface of magnetic nanoparticles (MNPs) were prepared. Three widely used functional monomers 2-(trifluoromethyl) acrylic acid (TFMAA), acrylic acid (AA), and methacrylic acid (MAA) were compared theoretically as the candidates for MIP preparation. MIP-coated magnetic nanoparticles (MIP-coated MNPs) showed large adsorption capacity, high recognition ability, and fast binding kinetics for tadalafil. Furthermore, because of the good magnetic properties, MIP-coated MNPs can achieve rapid and efficient separation with an external magnetic field simply. The resulting MIP-coated MNPs were used as dispersive solid-phase extraction (DSPE) materials coupled with HPLC-UV for the selective extraction and detection of tadalafil from medicines (herbal sexual health products). Encouraging results were obtained. The amounts of tadalafil that were detected from the herbal sexual health product was 43.46 nmol g<sup>-1</sup>, and the recoveries were in the range of 87.36–90.93% with the RSD < 6.55%.

**KEYWORDS:** magnetic molecularly imprinted polymers, PDE-5 inhibitors, tadalafil, medicines, HPLC-UV

## 1. INTRODUCTION

Tadalafil (Cialis) is a new oral selective phosphodiesterase-5 (PDE-5) inhibitor marketed for the improvement of erectile dysfunction (ED), which cleaves cyclic guanosine monophosphate (cGMP).<sup>1–3</sup> The drug works by suppressing the enzyme that controls blood flow, allowing the vessels to relax and widen. The same mechanism facilitates blood flow into the penis of impotent men. The usage of these PDE-5 inhibitors is controlled through medical supervision because of their harmful side-effects such as headache, dyspepsia, back pain, rhinitis, flu syndrome, etc.<sup>4</sup> These negative aspects of synthetic PDE-5-inhibitor drugs have triggered the development of herbal alternatives for the problem. These herbal therapies have been successful in capturing the market under the impression that they were safe and free from any side effects. However, many of them have been found subsequently containing synthetic PDE-5 inhibitors as adulterants. There have been reported that not only the approved drugs, but even unapproved analogues of PDE-5 inhibitors have been found in herbal aphrodisiacs.<sup>5–7</sup> The illegal products may endanger people's health.

The most common methods for the analysis of tadalafil in herb products reported were LC-MS, LC-MS/MS,<sup>8,9</sup> immunoassay,<sup>10</sup> and the combination of various methods.<sup>11</sup> Although these methods have good precision and sensitivity, all have their own shortcomings such as expensive equipment, trivial operation, need for professional operators. To determine substances in complex matrices, in order to avoid the interference of matrix effects, sample handling is critical. Good sample preparation methods can reduce the matrix effect interference and increase sensitivity. In all of these methods, they adopted the traditional sample processing methods, which were cumbersome and not selective.

A selective, accurate, and sensitive analytical method for detecting tadalafil in herbal sexual health products is important for the investigation of potential use of PDE-5 inhibitors in drug-safety field. The trace analysis of herbal complex samples generally needs a pretreatment step in order to reduce the matrix interference and enrich the analyte. Molecular imprinting is an increasingly applied technique to build selective recognition sites in a stable polymer matrix. MIPs having prearranged structure and specific molecular recognition abilities have been successfully applied to the separation and enrichment of analytes.<sup>12–20</sup> In addition, MIPs have found wide applications in chromatographic separation,<sup>21</sup> sensors,<sup>22–24</sup> solid-phase extraction (SPE),<sup>25,26</sup> solid-phase microextraction (SPME),<sup>27–29</sup> DSPE,<sup>12–14</sup> and other fields.<sup>30,31</sup>

In recent years, MNPs have been studied for biomedical and biotechnological applications. Magnetic separation technology has received considerable attention because of its potential application in cell isolation, enzyme immobilization, protein separation etc. A unique and attractive property of this technology is that magnetic supports can be isolated from sample solutions by the application of an external magnetic field. Therefore, when MNPs are coated with MIPs, these suspended MIP-coated MNPs can not only selectively recognize the analytes in the complex matrix, but also can be easily isolated from large volume samples by a magnet.<sup>32</sup> Because of the magnetic separation process can be performed directly in crude samples, which is especially useful for large-scale operation combining magnetic separation and molecular imprinting, would ideally provide a

**Received:** March 6, 2011

**Accepted:** August 28, 2011

**Published:** August 29, 2011

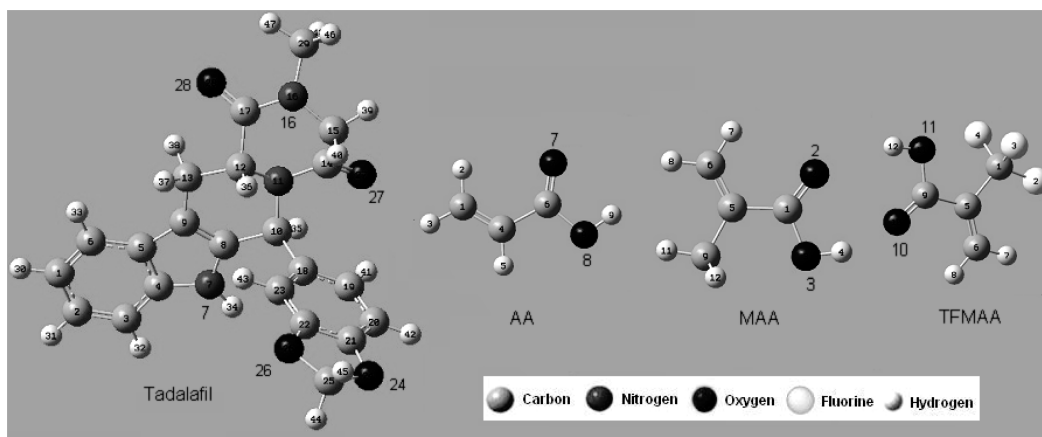


Figure 1. Optimized conformations of tadalafil, AA, MAA, and TFMAA.

powerful analytical tool toward selective and rapid application. Nowadays, some magnetic molecularly imprinted nanoparticles have been reported in the literature.<sup>23,33–35</sup>

Herein, highly selective MIPs for tadalafil were synthesized by molecular imprinting technique on the supporter of MNPs. We used quantum chemical computation to investigate into the synthesis of MIPs. As a combination of molecular imprinting technology the most prominent advantage of the material is that it has good selectivity and enrichment effects. The use of this material for sample pretreatment can be achieved detection of target molecular in complex samples. On the other hand, magnetic separation can be used to replace trivial filtration and centrifuge steps. Experimental results demonstrated that MIP-coated MNPs are selective toward the target molecules and achieve a rapid separation and enrichment because the efficient magnetic separation. Finally, we used MIP-coated MNPs as DSPE materials (MIP-coated MNPs-DSPE) coupled with HPLC-UV for the selective monitoring of trace tadalafil in herbal sexual health products. Encouraging results were obtained. To the best of our knowledge, this article was the first attempt to synthesize the magnetic molecularly imprinted nanoparticles for recognition of tadalafil.

## 2. EXPERIMENTAL SECTION

**2.1. Materials.** Sildenafil, vardenafil, and tadalafil were purchased from Zhengzhou Lion Biological Technology Co., Ltd., 2, 2'-Azobisisobutyronitrile (AIBN) was purchased from Shanghai No.4 Reagent & H.v Chemical Co., Ltd.,  $\gamma$ -methacryloxypropyl trimethoxysilane (MPTS) was obtained from Diamond Advanced Material of Chemical Inc., 2-(trifluoromethyl) acrylic acid (TFMAA) was from Shanghai Enfujia Technology Co., Ltd., ethylene glycol dimethacrylate (EGDMA) was purchased from Sigma-Aldrich Inc., tetraethyl orthosilicate (TEOS) was from Sinopharm Chemical Reagent Co., Ltd., all other chemicals used were of analytical grade and obtained commercially.

**2.2. Instrumentation.** HPLC was performed with a Shimadzu (Japan) system comprising LC-10ATVP pump, SPD-10AVP UV-detector and HW-2000 chromatographic workstation, detection wavelength was 230 nm. A Diamonsil C18 column (5  $\mu$ m, 150 mm  $\times$  4.6 mm) was used for above chromatographic experiments. The mobile phase consisted of methanol/water (60:40, v/v) at a flow rate of 1.0 mL  $\text{min}^{-1}$ . The injection volume was 20  $\mu$ L. Identification of target compounds was performed using an Agilent 1200 liquid chromatograph

Table 1. Binding Energies  $\Delta E$  of Tadalafil with MAA, AA, and TFMAA

molecules	mole ratio	energy (a.u.)	$\Delta E$ (a.u.)	$\Delta E$ (kJ $\text{mol}^{-1}$ )
tadalafil		-1290.6304		
AA		-262.1664		
MAA		-300.7518		
TFMAA		-593.1318		
complex (AA)	1:4	-2339.3312	0.0352	92.3984
complex (MAA)	1:4	-2493.6686	0.0310	81.3736
complex (TFMAA)	1:4	-3663.1970	0.0394	103.4233

which was coupled to an Agilent 6410B Triple Quad mass spectrometer. Other instruments used included Milli-Q (Millipore Co. Milford, MA, USA) water purification system, HZ-9211KB rocking bed (Hualida Laboratory Equipment Co., Ltd.), C-MAG HS 7 Temperature magnetic mixer (IKA Processing Equipment, Germany), KQ5200 Ultrasonic Cleaner (Kunshan Ultrasonic Instrument Co., Ltd., China), DZG-6020 vacuum drying oven (Shanghai Sumsung Laboratory Equipment Co., Ltd., China), JSM-5900 scanning electron microscope (SEM) (JEOL Ltd., Japan), JEM1010 transmission electron microscope (TEM) (JEOL Ltd., Japan), Malvern zetasizer nano series (Malvern instruments Ltd.), M27407 vibrating sample magnetometry (VSM) (Lake Shore Ltd.), Rigaku D/max22500 X-ray diffraction (XRD) (Rigaku Ltd., Japan).

**2.3. Samples.** Herbal sexual health products (The obtained samples have the following active principle and composition, as described by the manufacturer: Radix Ginseng, Colla Comus Cervi, Lycium chinense mill, Herba Cistanches Deserticolae, Radix Morindae Officinalis, Semen Trigonellae, Poria, Fructus Hippophae, Fructus Schisandrae Chinensis, Cortex Acanthopanax Radicis, Herba Scutellariae Barbatae, and so on.) were purchased from the market. The manufacturer was Dadi Co., Ltd.

**2.4. Choice of Functional Monomers.** Simulation of interactions between tadalafil and monomers (AA, MAA and TFMAA) was performed using the ab initio 3-21G basis set (HF/3-21G) at the Hartree–Fock (HF) level with the Gaussian 09 software. The conformations of them were optimized and the energy of the molecules with the optimized conformation was calculated. The electronic energies between template and monomer were calculated through semiempirical quantum methods (PM3). The binding energy ( $\Delta E$ ) was finally computed by the following generic formula:  $\Delta E = |E_{\text{complex}} - E_{\text{template}} - E_{\text{monomer}}|$

**2.5. Choice of Solvent.** Because all noncovalent forces are significantly influenced by the properties of solvent,<sup>36</sup> various solvents

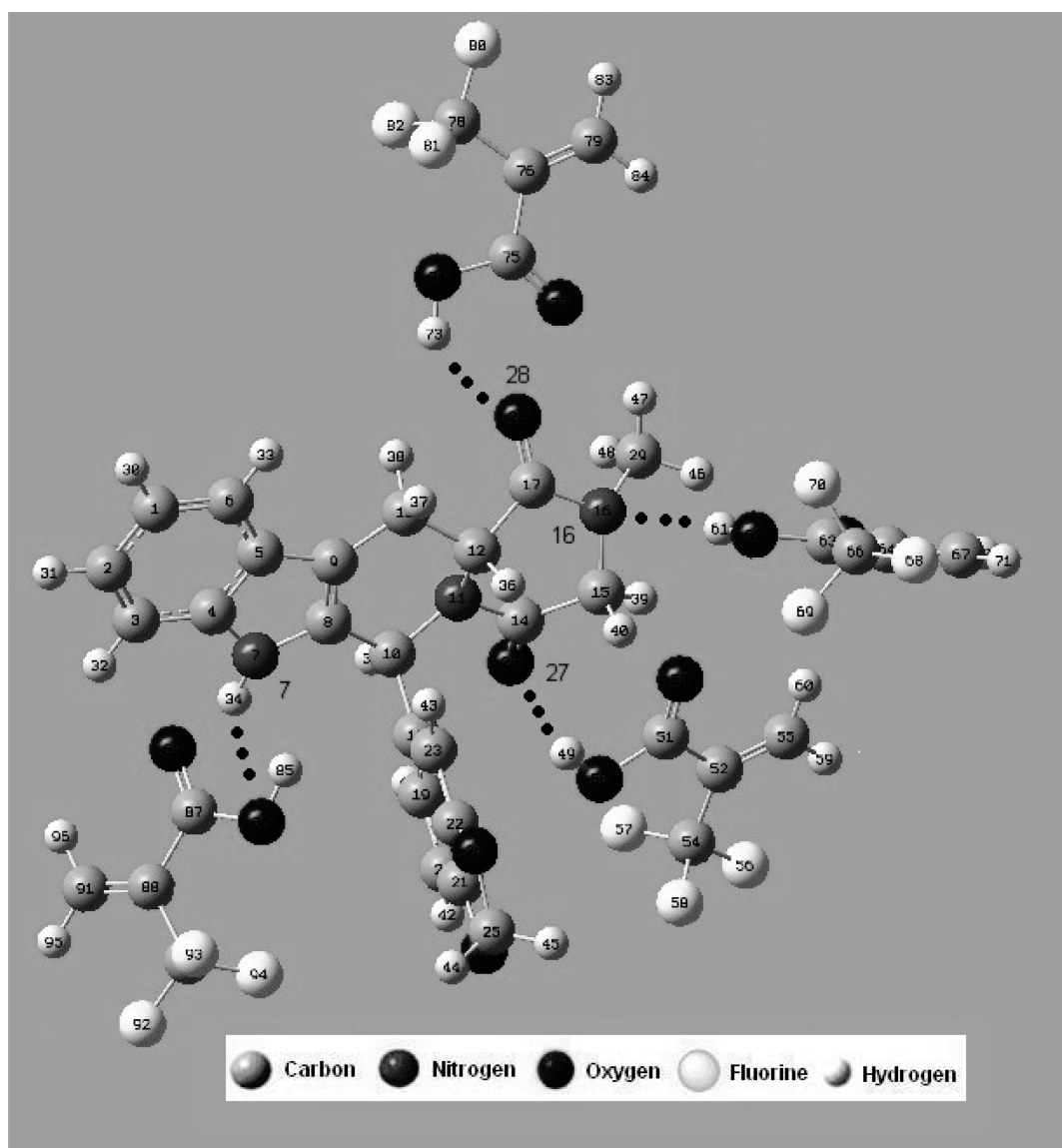


Figure 2. Predicted structure of the complex formed between tadalafil and TFMAA.

including water ( $\text{H}_2\text{O}$ ), methanol ( $\text{MeOH}$ ), acetonitrile ( $\text{ACN}$ ), ethanol ( $\text{EtOH}$ ), chloroform ( $\text{TCM}$ ), dichloromethane ( $\text{DCM}$ ), and toluene ( $\text{PhMe}$ ) were investigated through Gaussian 09 software to choose an ideal rebinding solvent.

**2.6. Preparation of Surface-Modified  $\text{Fe}_3\text{O}_4@/\text{SiO}_2$  Nanospheres.** Iron oxide nanoparticles were first synthesized by solvothermal reduction method and  $\text{Fe}_3\text{O}_4@/\text{SiO}_2$  was synthesized by hydrolysis of TEOS with aqueous ammonia<sup>20–23</sup> as follows: 1.72 g of  $\text{FeCl}_2 \cdot 4\text{H}_2\text{O}$  and 4.72 g of  $\text{FeCl}_3 \cdot 6\text{H}_2\text{O}$  were dissolved in 80 mL of water in a three-necked reactor. The mixture was stirred equably and purged with nitrogen gas until the temperature increased to 80 °C, and then 10 mL of aqueous ammonia was added into it. This reaction lasted 1 h at 80 °C. When the temperature dropped to room temperature, the magnetic precipitates obtained were isolated from the solution by an external magnetic field and washed with deionized water several times until it was neutral. Then surface modified  $\text{Fe}_3\text{O}_4@/\text{SiO}_2$  nanospheres were prepared. In short, 2 mL of MPTS was added to a suspension of 0.1 g of  $\text{Fe}_3\text{O}_4@/\text{SiO}_2$  nanospheres in 50 mL of toluene under the protecting of nitrogen. The mixture was stirred 24 h at 120 °C. The product was collected by an external magnetic field and dried in a vacuum.

**2.7. Preparation of MIP-Coated MNPs.** MIP-coated MNPs were prepared by precipitation polymerization using tadalafil, TFMAA, EGDMA and AIBN as template molecule, functional monomer, cross-linker, and initiator, respectively. 0.26 mmol tadalafil, 1.04 mmol TFMAA and 40 mg modified  $\text{Fe}_3\text{O}_4@/\text{SiO}_2$  nanospheres were dispersed into 50 mL of toluene, the mixture was stirred 1 h at room temperature to facilitate the combination between template molecule and functional monomer. Then, 2.08 mmol of cross-linker and 20 mg of initiator were added to above mixture. Under the protecting of nitrogen, the mixture was stirred 6 h at 50 °C, 24 h at 60 °C, and 8 h at 85 °C. Nonimprinted polymers coated magnetic nanoparticles (NIP-coated MNPs) were prepared identically except for the addition of template molecules.

The polymers were separated by an external magnetic field, washed with a mixture of methanol and acetic acid (9:1, v/v) to extract the template molecules until there was no tadalafil that could be detected by UV spectrometer in the rinses. The obtained polymers were finally rinsed with methanol to remove the remaining acetic acid and then dried in the vacuum desiccators for 24 h before used.

**2.8. Characterization of MIP-Coated MNPs.** The size and magnetic properties of MIP-coated MNPs were characterized by TEM

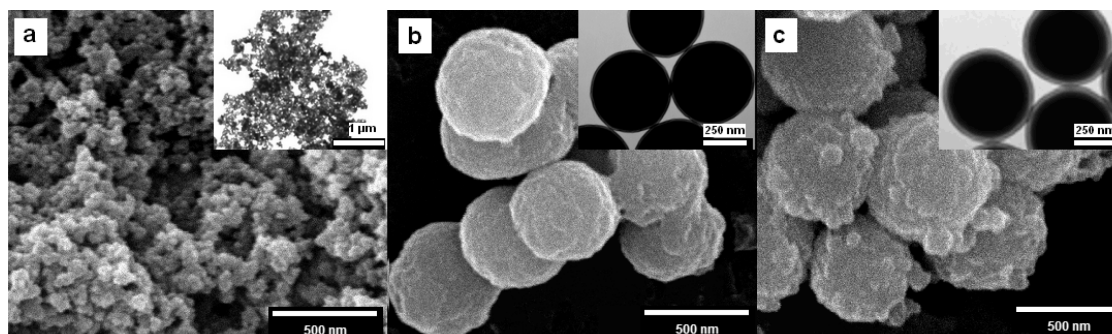


Figure 3. SEM and TEM (the insets) images of (a)  $\text{Fe}_3\text{O}_4$ , (b)  $\text{Fe}_3\text{O}_4@\text{SiO}_2$ , and (c) MIP-coated MNPs.

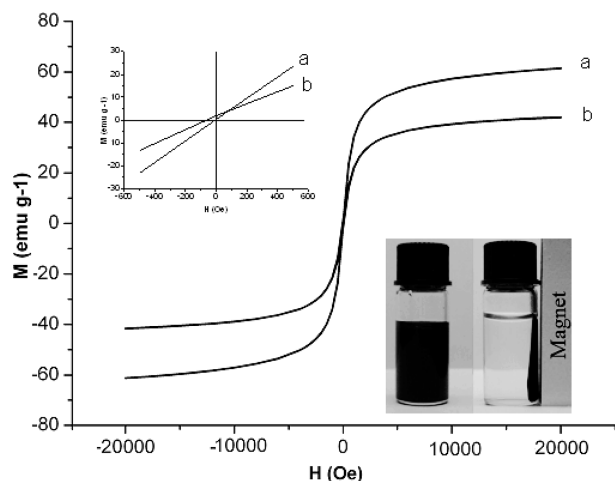


Figure 4. VSM analysis of (a)  $\text{Fe}_3\text{O}_4@\text{SiO}_2$  and (b) MIP-coated MNPs.

and VSM respectively. The identification of crystalline phase of MIP-coated MNPs was performed using an XRD over the  $2\theta$  range of  $10\text{--}80^\circ$ .<sup>37,38</sup>

**2.9. Binding Experiment.** To evaluate the recognition properties of MIPs toward the target molecule, we carried out dynamic and static adsorption tests according to the reported methods.<sup>11</sup> The static adsorption was measured by suspending 20 mg of MIP-coated MNPs in 2 mL of toluene/methanol (5:5, v/v) with different tadalafil concentrations ( $0.06\text{--}5\text{ mmol L}^{-1}$ ). Meanwhile, the dynamic adsorption was tested by detecting the temporal evolution of tadalafil concentration ( $2\text{ mmol L}^{-1}$ ) in the solutions. The concentrations of tadalafil were monitored by HPLC via UV detection at 230 nm.

The selectivity of MIP-coated MNPs was investigated using the analogues of tadalafil (sildenafil and vardenafil). NIP-coated MNPs were used for comparison.

**2.10. Detection of Tadalafil in Herbal Sexual Health Products.** Calibration was made by the standard curve method. The calibration curve was constructed by measuring five different concentrations of estrogens ranging from  $0.0980$  to  $1.96\text{ }\mu\text{g mL}^{-1}$ . For recovery studies, real samples spiked with tadalafil in three different levels were treated and tested by the method built. One hundred milligrams of pestled samples were mixed with three levels of tadalafil standard solutions, respectively.

MIP-coated MNPs-DSPE coupled with HPLC-UV was developed to determine tadalafil in real samples. One hundred milligrams of pestled samples were vortex-mixed with 10 mL of acetonitrile and ultrasounded for 20 min. After that, the mixture was separated by filtrating, and the

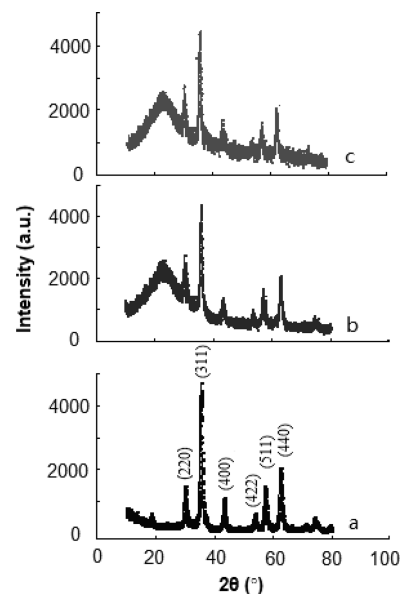


Figure 5. X-ray diffraction patterns of (a)  $\text{Fe}_3\text{O}_4$ , (b)  $\text{Fe}_3\text{O}_4@\text{SiO}_2$  and (c) MIP-coated MNPs.

filtrate was kept. One milliliter of filtrate was evaporated under nitrogen gas at room temperature, 20 mg of MIP-coated MNPs was added to the residue, the mixture was reconstituted with 1 mL of toluene/methanol (5:5, v/v) and shaken at room temperature for 15 min, and MIP-coated MNPs were separated by an external magnetic field and then washed with 1 mL of methanol/acetic acid (9:1, v/v) by sonication for 12 min. Eight-tenths of a milliliter of supernatants was obtained and evaporated to dryness under nitrogen gas at  $40^\circ\text{C}$ . Finally, the residues were redissolved in 0.8 mL of mobile phase for further HPLC-UV analysis.

### 3. RESULTS AND DISCUSSION

**3.1. Choice of Functional Monomers.** The selection of the suitable functional monomers is a crucial factor in the study of MIPs. In this work, three widely used functional monomers AA, MAA, and TFMAA were compared theoretically. The optimized conformations of tadalafil and the three functional monomers were shown in Figure 1.

We compared the Mulliken charges of the atoms in tadalafil, AA, MAA, and TFMAA. From the results the results and the spatial considerations, we deduced that the proton donor in tadalafil was  $\text{N}_7$  and the proton acceptors were  $\text{N}_{16}$ ,  $\text{O}_{27}$ , and  $\text{O}_{28}$ . For TFMAA, the proton donor was  $\text{H}_{12}$  and the proton acceptor

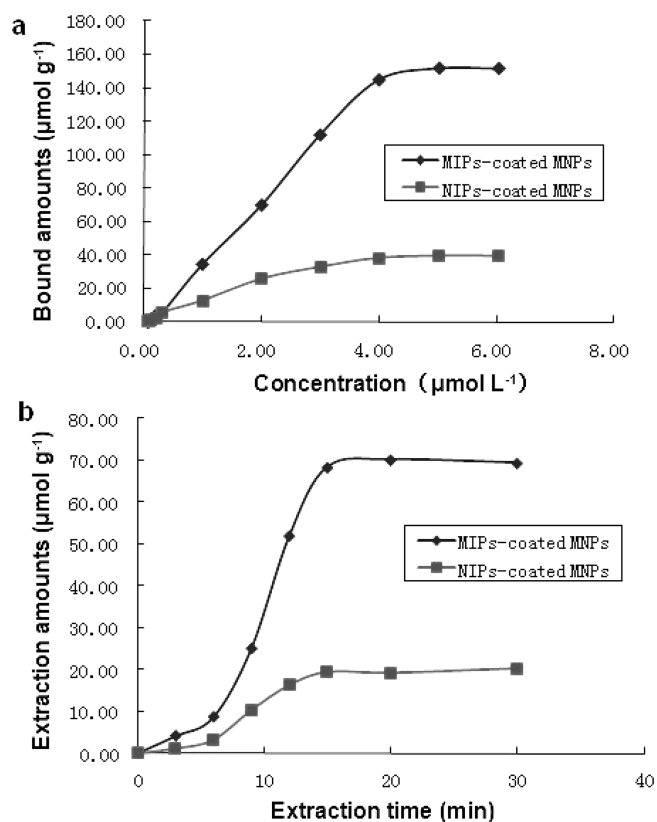


**Figure 6.** (a) Static and (b) dynamic adsorption curve for MIP-coated MNPs (◆) and NIP-coated MNPs (■) respectively.

was  $O_{11}$ . In addition, we calculated the binding energy ( $\Delta E$ ) of complexes between tadalafil and monomers. Various binding sites and their combination were compared. Table 1 showed that  $\Delta E$  (TFMAA) >  $\Delta E$  (MAA) >  $\Delta E$  (AA), indicating that TFMAA giving the highest binding energy is more likely to form strong complexes with tadalafil. Figure 2 showed the Gaussian predicted structure of the complex formed between the tadalafil molecule and four molecules of TFMAA.

**3.2. Choice of Solvent.** Figure S1 in the Supporting Information shows toluene is the best one in simulation of synthesis complex in different solvent. So, toluene was chosen as the solvent in the later experiments.

**3.3. Preparation of MIP-Coated MNPs.** MIP-coated MNPs were prepared as mentioned above. The affinity and imprinting effect of the MIP-coated MNPs were affected by the molar ratios between the functional monomer and cross-linker. Therefore, four molar ratios between the functional monomer and cross-linker of 1:1, 1:2, 1:4 and 1:8 were tested in the experiment. The results in Figure S2 in the Supporting Information revealed that the MIP-coated MNPs had high adsorption capacity and selectivity with the molar ratios of 1:2, while other molar ratios showed low adsorption capacity and selectivity. It can be explained that if there is too little cross-linker, then the cross-linking is not enough, and effective imprinting sites can not be formed. On the other hand, too much cross-linker will lead to the template molecules being embedded too deeply and will reduce effective imprinting sites. After the residues of tadalafil were removed, a large number of tailor-made cavities for tadalafil on the surface of magnetic silica nanoparticles were formed.

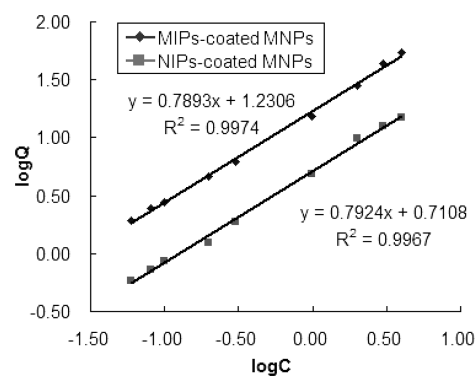


**Figure 7.** Adsorption isotherm of tadalafil fitting to the Freundlich isotherm on MIP-coated MNPs and NIP-coated MNPs.

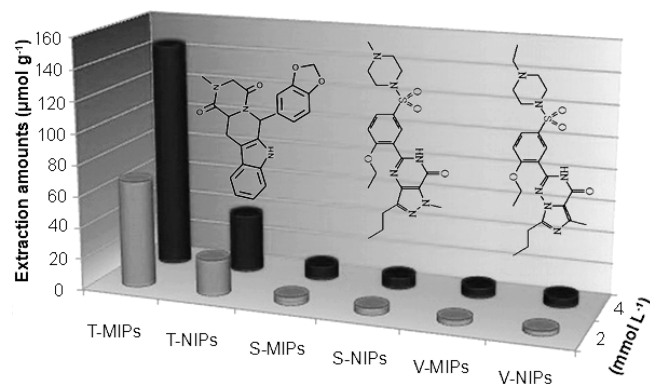
**3.4. Characterizations of MIP-Coated MNPs.** In Figure 3, the scanning electron micrographs and transmission electron micrographs of nanoparticles taken at various stages of preparation were shown. Figure 3a showed the SEM and TEM images of the  $Fe_3O_4$  nanoparticles. This image reveals the obtained  $Fe_3O_4$  nanoparticles were spherical in shape. Because of their size was very small, so it is easy to assemble together. The diameter was about 30 nm. Figure 3b showed the SEM and TEM images of  $Fe_3O_4@SiO_2$ . It can be seen that the magnetic nanoparticles were fully coated by silica. The particles were size uniform, and the morphology of particles was highly spherical. Figure 3c clearly showed MIP-coated MNPs. Compared with Figure 3b, the SEM micrographs in c showed relatively rough and well-clustered micro islands, suggesting the formation of imprinting layer. The TEM micrographs clearly show the core-shell structure of MIP-coated MNPs. The polymer shell became thicker than  $Fe_3O_4@SiO_2$ , which is the result of the formation of imprinting layer. Dynamic light scattering (DLS) was employed to characterize the size and dispersion of nanoparticles. The average particle sizes for  $Fe_3O_4@SiO_2$  and MIP-coated MNPs were 470.7 and 515.2 nm and the polydispersity index (PDI) were 0.278 and 0.314, respectively.

The magnetization curves (Figure 4) of VSM analysis showed the saturation magnetization of  $Fe_3O_4@SiO_2$  (curve a) and MIP-coated MNPs (curve b) were about 61 and 42  $emu\ g^{-1}$ , respectively. The existence of MIPs on the surface of  $Fe_3O_4@SiO_2$  nanoparticles most likely contributes to the decrease of the saturation magnetization. The inset in the upper-left corner was the detailed view of x and y intercepts of the graph. It was apparent that both remanence and coercivity were relatively low. It may be attributed to the size of  $Fe_3O_4$  wrapped in these nanoparticles was small enough. This suggested that the materials could respond magnetically to an external magnetic field effectively and could well disperse when removal of the field. The picture inserted in the bottom right corner of Figure 4 showed the separation and redispersion process of MIP-coated MNPs in the presence and absence of an external magnetic field, respectively. In the absence of an external magnetic field, a homogeneous dispersion was demonstrated. When an external magnetic field was applied, the particles were attracted to the wall of vial in a short time (about 10 s).

Figure 5 showed the X-ray diffraction (XRD) patterns for,  $Fe_3O_4$  (curve a),  $Fe_3O_4@SiO_2$  (curve b) and MIP-coated MNPs (curve c). It revealed that the synthesized process essentially did

**Table 2.** Freundlich Fitting Parameters, Weighted Average Affinity, And Number of Sites for MIP-Coated MNPs and NIP-Coated MNPs

	$m$	$\alpha$ ((mg g <sup>-1</sup> ) (L g <sup>-1</sup> ) <sup>m</sup> )	$R^2$	$N_{K_{\min}-K_{\max}}$ (mg g <sup>-1</sup> )	$\bar{K}_{K_{\min}-K_{\max}}$ (mL g <sup>-1</sup> )
MIP-coated MNPs	0.79	17.01	0.9974	10.23	2.92
NIP-coated MNPs	0.79	5.14	0.9967	2.26	1.32

**Figure 8.** Selective recognition property of MIP-coated MNPs and NIP-coated MNPs with tadalafil (T), sildenafil (S), and vardenafil (V) at levels of 2 and 4 mol L<sup>-1</sup>.

not change the XRD phase of Fe<sub>3</sub>O<sub>4</sub>. The diffraction peak 10–30° is the amorphous diffraction of SiO<sub>2</sub>.

**3.5. Evaluation of the Adsorption Characteristic of MIP-Coated MNPs.** The binding isotherm of tadalafil onto tadalafil-imprinted sorbent was shown as Figure 6a. It exhibited MIP-coated MNPs had much stronger memory function and higher adsorption capacity for the template than NIPs. The static adsorption capacities of MIP-coated MNPs and nonimprinted sorbents for tadalafil were calculated as 152 and 39.31 µmol g<sup>-1</sup>, respectively. Stability and recovery were calculated. Five batches of MIP-coated MNPs and NIP-coated MNPs were investigated to compare their adsorption capacity and imprinting factor and the RSD were 2.65 and 5.72% respectively, confirming that the preparation method was highly reproducible.

The adsorption kinetics of MIP-coated MNPs was investigated with 2 mmol L<sup>-1</sup> tadalafil solution at different time intervals. The binding sites of MIP-coated MNPs were produced on the surface or in the proximity of the surface. This will help the target to access or dissociate the recognition sites easily. As shown in Figure 6b MIP-coated MNPs had fast adsorption kinetics within approximately 15 min. This merit is especially propitious to detect analytes faster.

The Freundlich isotherm (FI) model was used to account for heterogeneous binding sites in imprinted polymers. It is expressed by eq 1.

$$Q = \alpha C^m \quad (1)$$

Where  $Q$  and  $C$  are the concentrations of bound and free analyte, respectively and  $\alpha$  and  $m$  are fitting constants that have physical meaning. Freundlich constants  $\alpha$  and  $m$  could be calculated by plotting  $\log Q$  versus  $\log C$  by a linear regression as eq 2.

$$\log Q = \log \alpha + m \log C \quad (2)$$

**Table 3.** Result of Detection of Tadalafil in Herbal Sexual Health Product

compd	content in real sample (nmol/g)	spiked amount (nmol/g)	recovery/R.SD. (%), $n = 3$	linearity ( $r$ , $n = 6$ )
tadalafil	43.46	20.38	87.36	6.55
		40.77	89.93	4.27
		61.16	90.93	3.44

The apparent number of binding sites per gram of material ( $N_{K_{\min}-K_{\max}}$ ), and the apparent average association constant ( $\bar{K}_{K_{\min}-K_{\max}}$ ), calculated using eqs 3 and 4.

$$N_{K_{\min}-K_{\max}} = \alpha(1 - m^2)(K_{\min}^{-m} - K_{\max}^{-m}) \quad (3)$$

$$\bar{K}_{K_{\min}-K_{\max}} = \left( \frac{m}{m-1} \right) \left( \frac{K_{\min}^{1-m} - K_{\max}^{1-m}}{K_{\min}^{-m} - K_{\max}^{-m}} \right) \quad (4)$$

The information showed all the experimental data of this study (see Figure 7), which are summarized in Table 2.

The data also showed that  $N_{K_{\min}-K_{\max}}$  in MIP-coated MNPs was much higher than in NIP-coated MNPs. This means that the number of sites with adequate geometry and good accessibility to tadalafil were higher in MIP-coated MNPs than in NIP-coated MNPs, demonstrating the imprinting phenomenon.

The selectivity test results among different compounds may also show some aspects of molecular recognition. Figure 8 demonstrated that tadalafil-imprinted polymer-coated MNPs exhibited high selectivity for imprinting molecule tadalafil compared to the analogues sildenafil and vardenafil. The controlled NIPs showed low binding values for all of them. The results confirmed clearly the effectiveness of the molecular imprinting because the tadalafil-imprinted MNPs showed efficiently specific recognition ability to the template in comparison with analogues.

**3.6. Method Validation.** Good linearity was achieved in range of 0.098–1.96 µg mL<sup>-1</sup> for tadalafil with correlation coefficient of 0.9987. Nine successive measurements of tadalafil in real sample using the same one MIP-coated MNPs-DSPE yielded an RSD of 4.43%, indicating that the cleanup system was stable.

**3.7. Sample Analysis.** The established MIP-coated MNPs-DSPE coupled with HPLC-UV method was applied to analysis of tadalafil in herbal sexual health product. The recoveries and reproducibility of the method were calculated and summarized in Table 3. As can be seen, the tadalafil recoveries were in the range of 87.36–90.93% with the RSD < 6.55%.

Figure 9a showed HPLC chromatograms of tadalafil in herbal sexual health products by direct injection (curve a), extracted by MIP-coated MNPs (curve c) and NIP-coated MNPs (curve d) and spiked tadalafil (20.38 nmol g<sup>-1</sup>) extracted by MIP-coated MNPs (curve b). The result revealed that tadalafil in herbal sexual health products could not be detected by HPLC-UV without enrichment, whereas it can be quantitated after being extracted with MIP-coated MNPs. Moreover, the baseline noises in the MIP-coated MNP-DSPE method were much less than others. Most interfering compounds in herbal sexual health products were successfully cleaned up after being extracted with MIP-coated MNP-DSPE, thus allowing the extraction of tadalafil with high selectivity. The curve d showed no such selectivity with NIP-coated MNP-DSPE protocol. The amount of tadalafil detected from the

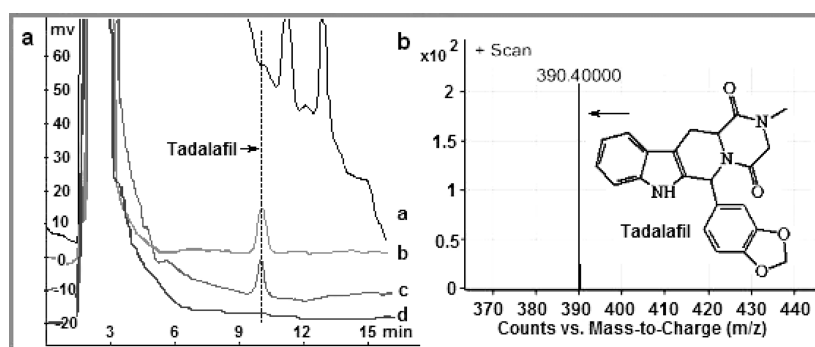


**Figure 9.** (a) HPLC chromatograms of tadalafil in the herbal sexual health product by direct injection (curve a), extracted by MIP-coated MNPs (curve c) and NIP-coated MNPs (curve d), the spiked tadalafil ( $20.38 \text{ nmol g}^{-1}$ ) extracted by MIP-coated MNPs (curve b). (b) Validation of the target compounds in samples by HPLC-MS/MS.

sample was  $43.46 \text{ nmol g}^{-1}$ . The target compounds in the obtained solution as mentioned above had been identified by HPLC-MS/MS (Figure 9b).

The results demonstrated that MIP-coated MNPs had high selectivity and enrichment ability. Because of the selective binding sites at the surface of MIP-coated MNPs nanoparticles, MIP-DSPE can reach the equilibrium quickly. Furthermore, because of the good magnetic properties, MIP-coated MNPs can achieve rapid and efficient separation with an external magnetic field simply. The MIP-coated MNP-DSPE process does not require a special instrument, consumes much less toxic organic solvent, reduces the loss of adsorbent, and has good cleanup and concentration effect for the analytes. Hence, the tadalafil-imprinted nanoparticles can be offered as a simple and straightforward technique for the direct analysis of tadalafil from the complicated matrices without lengthy sample cleanup.

#### 4. CONCLUSIONS

In conclusion, we developed an efficient method for preparation of magnetic molecularly imprinted nanoparticles. Computational approaches using the binding energy ( $\Delta E$ ) and Mulliken charges were used to select and determine the molar ratio of functional monomer. The structure of the complex formed between tadalafil and TFMAA was predicted. The resulting MIP-coated MNP nanoparticles exhibited good characteristics, such as highly spherical and uniform morphology, smooth surface, superior selectivity, and good reproducibility. It was successfully used as DSPE materials to selectively enrich and determine tadalafil in herbal sexual health products. Magnetic separation had been used to replace filtration and centrifuge steps. The results exhibited high recovery, precision, and sensitivity. The proposed method provides an effective tool for the monitoring of tadalafil in the sexual health product-safety field. Therefore, the novel approach is well-suited to be exploited in enrichment and detection of trace analytes in many complicated matrices.

#### ASSOCIATED CONTENT

**Supporting Information.** Additional figures (PDF). This material is available free of charge via the Internet at <http://pubs.acs.org/>.

#### AUTHOR INFORMATION

##### Corresponding Author

\*Tel: + 86 25 86862762. Fax: + 86 25 86862762. E-mail: zxm001\_001@yahoo.cn.

##### Author Contributions

<sup>†</sup>Yun Li and Mei-juan Ding contributed equally to this work.

#### ACKNOWLEDGMENT

This work was supported by National Natural Science Foundation of China (20875048, 21175070), Natural Science Foundation of Jiangsu Province (BK2008439) and University Students' Practice Innovation Training Project Funds of Jiangsu Province (KY109J2010001).

#### REFERENCES

- (1) Ormrod, D.; Easthope, S. E.; Figgitt, D. P. *Drugs Aging* **2002**, *19*, 217.
- (2) Briganti, A.; Salonia, A.; Gallina, A.; Sacca, A.; Montorsi, P.; Rigatti, P.; Montorsi, F. *Nat. Clin. Pract. Urol.* **2005**, *2*, 239.
- (3) Gupta, M.; Kova, A.; Melbohm, B. *J. Clin. Pharmacol.* **2005**, *45*, 987.
- (4) Porst, H. *EAU Update Series* **2004**, *2*, 56.
- (5) Singh, S.; Prasad, B.; Savaliya, A. A.; Shah, R. P.; Gohil, V. M.; Kaur, A. *Trends Anal. Chem.* **2009**, *28*, 13.
- (6) Venhuis, B. J.; Zomer, G.; de Kaste, D. *J. Pharm. Biomed. Anal.* **2008**, *46*, 814.
- (7) Reepmeyer, J. C.; d'Avignon, D. A. *J. Pharm. Biomed. Anal.* **2009**, *49*, 145.
- (8) Bogusz, M. J.; Hassan, H.; Al-Enazi, E.; Ibrahim, Z.; Al-Tufail, M. *J. Pharm. Biomed. Anal.* **2006**, *41*, 554.
- (9) Zhu, X. L.; Xiao, S.; Chen, B.; Zhang, F.; Yao, S. Z.; Wan, Z. T.; Yang, D. J.; Han, H. W. *J. Chromatogr. A* **2005**, *1066*, 89.
- (10) Guo, J. B.; Xu, Y.; Huang, Z. B.; He, Q. H.; Liu, S. W. *Anal. Chim. Acta* **2010**, *658*, 197.
- (11) Gratz, S. R.; Flurer, C. L.; Wolnik, K. A. *J. Pharm. Biomed. Anal.* **2004**, *36*, 525.
- (12) Wang, S.; Li, Y.; Wu, X. L.; Ding, M. J.; Yuan, L. H.; Wang, R. Y.; Wen, T. T.; Zhang, J.; Chen, L. N.; Zhou, X. M.; Li, F. *J. Hazard. Mater.* **2011**, *186*, 1513.
- (13) Ma, J.; Yuan, L. H.; Ding, M. J.; Wang, S.; Ren, F.; Zhang, J.; Du, S. H.; Li, F.; Zhou, X. M. *Biosens. Bioelectron.* **2011**, *26*, 2791.
- (14) Lu, Q.; Chen, X. M.; Nie, L.; Luo, J.; Jiang, H. J.; Chen, L. N.; Hu, Q.; Du, Sh., H.; Zhang, Z. P. *Talanta* **2010**, *81*, 959.
- (15) Zhou, W. H.; Lu, C. H.; Guo, X. C.; Chen, F. R.; Yang, H. H.; Wang, X. R. *J. Mater. Chem.* **2010**, *20*, 880.

- (16) Zhang, Y.; Li, Y. W.; Hu, Y. L.; Li, G. K.; Chen, Y. Q. *J. Chromatogr., A* **2010**, *1217*, 7337.
- (17) Gai, Q. Q.; Qu, F.; Liu, Z. J.; Dai, R. J.; Zhang, Y. K. *J. Chromatogr., A* **2010**, *1217*, 5035.
- (18) Wang, X.; Wang, L. Y.; He, X. W.; Zhang, Y. K.; Chen, L. X. *Talanta* **2009**, *78*, 327.
- (19) Li, L.; He, X. W.; Chen, L. X.; Zhang, Y. K. *Chem. Asian J.* **2009**, *4*, 286.
- (20) Chen, L. G.; Zhang, X. P.; Xu, Y.; Du, X. B.; Sun, X.; Sun, L.; Wang, H.; Zhao, Q.; Yu, A. M.; Zhang, H. Q.; Ding, L. *Anal. Chim. Acta* **2010**, *662*, 31.
- (21) Tamayo, F. G.; Martin-Esteban, A. J. *Chromatogr., A* **2005**, *1098*, 116.
- (22) Agostino, G. D.; Alberti, G.; Biesuz, R.; Pesavento, M. *Biosens. Bioelectron.* **2006**, *22*, 145.
- (23) Apodaca, D. C.; Pernites, R. B.; Ponnampati, R. R.; DelMundo, F. R.; Advincula, R. C. *ACS Appl. Mater. Interfaces* **2011**, *3*, 191.
- (24) Holthoff, E. L.; Bright, F. V. *Acc. Chem. Res.* **2007**, *40*, 756.
- (25) Caro, E.; Marcé, R. M.; Borrull, F.; Cormack, P. A. G.; Sherrington, D. C. *Trends Anal. Chem.* **2006**, *25*, 143.
- (26) Dias, A. C. B.; Figueiredo, E. C.; Grassi, V.; Zagatto, E. A. G.; Arruda, M. A. Z. *Talanta* **2008**, *76*, 988.
- (27) Mullett, W. M.; Martin, P.; Pawliszyn J. *Anal. Chem.* **2001**, *73*, 2383.
- (28) Hu, X. G.; Hu, Y. L.; Li, G. K. *J. Chromatogr. A.* **2007**, *1147*, 1.
- (29) Hu, X. G.; Pan, J. L.; Hu, Y. L.; Huo, Y.; Li, G. K. *J. Chromatogr., A* **2008**, *1188*, 97.
- (30) Paik, P.; Gedanken, A.; Mastai, Y. *ACS Appl. Mater. Interfaces* **2009**, *1*, 1834.
- (31) Balogh, D.; Tel-Vered, Ran.; Riskin, M.; Orbach, R.; Willner, I. *ACS Nano* **2011**, *5*, 299.
- (32) Campíns-Falcó, P.; Verdú-Andrés, J.; Sevillano-Cabeza, A.; Molins-Legua, C.; Herráez-Hernández, R. *J. Chromatogr., A* **2008**, *1211*, 13.
- (33) Jing, T.; Du, H. R.; Dai, Q.; Xia, H.; Niu, J. w.; Hao, Q. L.; Mei, S. R.; Zhou, Y. K. *Biosens. Bioelectron.* **2010**, *26*, 301.
- (34) Chen, L. G.; Liu, J.; Zeng, Q. L.; Wang, H.; Yu, A. M.; Zhang, H. Q.; Ding, L. *J. Chromatogr., A* **2009**, *1216*, 3710.
- (35) Aguilar-Arteaga, K.; Rodriguez, J. A.; Miranda, J. M.; Medina, J.; Barrado, E. *Talanta* **2010**, *80*, 1152.
- (36) An, F.; Gao, F.; Wang, X. *J. Hazard. Mater.* **2008**, *157*, 286.
- (37) Kowalska, A.; Stobiecka, A.; Wysocki, S. *J. Mol. Struct. Theor. Chem.* **2009**, *901*, 88.
- (38) Li, Y.; Li, X.; Chu, J.; Dong, C. k.; Qi, J. Y.; Yuan, Y. X. *Environ. Pollut.* **2010**, *158*, 2317.